



저작자표시-비영리-변경금지 2.0 대한민국

이용자는 아래의 조건을 따르는 경우에 한하여 자유롭게

- 이 저작물을 복제, 배포, 전송, 전시, 공연 및 방송할 수 있습니다.

다음과 같은 조건을 따라야 합니다:



저작자표시. 귀하는 원저작자를 표시하여야 합니다.



비영리. 귀하는 이 저작물을 영리 목적으로 이용할 수 없습니다.



변경금지. 귀하는 이 저작물을 개작, 변형 또는 가공할 수 없습니다.

- 귀하는, 이 저작물의 재이용이나 배포의 경우, 이 저작물에 적용된 이용허락조건을 명확하게 나타내어야 합니다.
- 저작권자로부터 별도의 허가를 받으면 이러한 조건들은 적용되지 않습니다.

저작권법에 따른 이용자의 권리는 위의 내용에 의하여 영향을 받지 않습니다.

이것은 [이용허락규약\(Legal Code\)](#)을 이해하기 쉽게 요약한 것입니다.

[Disclaimer](#)

Design of an Extremely Miniaturized Balun Filter Using Open-stubs for Harmonic Suppression

By YUZHE ZHANG

Under the Supervision of Prof. In-Ho Kang

Department of Radio Sciences and Engineering

in the Graduate School

of

Korea Maritime and Ocean University

May 2017

This thesis, which is an original work undertaken by YUZHE ZHANG in partial fulfillment of the requirements for the degree of Master of Radio Sciences and Engineering, is in accordance with the regulations governing the preparation of thesis at the Graduate School in the Korea Maritime and Ocean University, Republic of Korea.

Approved by the Thesis Committee:

Professor Yoon. Young _____
Chairman

Professor Kang. In Ho _____
Member

Professor Park. Dong Gook _____
Member

August 2017

the Graduate School of Korea Maritime and Ocean
University

Department of Radio Sciences and Engineering

Contents

Contents	I
Nomenclature	II
List of Tables	III
List of Figures	IV
Abstract	1
CHAPTER 1 Introduction	3
1.1 RF filter introduction and basic parameters.....	3
1.2 Background and Introduction of Balun.....	5
1.3 Organization of the Thesis.....	9
CHAPTER 2 Balun Filter Design Theory	11
2.1 Size Reduction Method.....	11
2.1.1 Diagonally Shorted Coupled Lines with Lumped Capacitors.....	12
2.1.2 Parallel End Shorted Coupled Lines with Lumped Capacitors.....	16
2.2 The Open-stub Equivalent Circuit.....	19
2.3 Ordinary Balun Design.....	21
2.4 New Structure for Miniaturized Balun Filter.....	24
CHAPTER 3 Simulation, Fabrication and Measurement	30
3.1 Circuit Simulating by ADS and Analysis.....	30
3.1.1 Circuit Simulating of original coupled line circuit.....	32
3.1.2 The equivalent Circuit Simulating by adding a open-stub to act in capacitive.....	34
3.2 Simulation by HFSS and Optimization.....	38
3.3 Fabrication and Measurement.....	42
Chapter 4 Conclusion	46
References	47
Acknowledgement	50

Nomenclature

Z_0	Characteristic impedance
Z_{oe}	Even-mode characteristic impedance
Z_{oo}	Odd-mode characteristic impedance
Y_0	Characteristic admittance
Y_{oe}	Even-mode characteristic admittance
Y_{oo}	Odd-mode characteristic admittance
θ	Electrical length
ω	Angular frequency
C	Capacitance
L	Inductance
S	Scattering parameter
T	Transmission coefficient

List of Tables

Table 3. 1 Ideal specifications of the proposed filter 30
Table 3. 2 Design parameters of the HFSS simulation 40



List of Figures

Fig. 1.1 A planar version of Marchand balun

Fig. 2.1 Quarter-wave transmission line (a) and its equivalent shorted transmission line circuit (b)

Fig. 2.2 Diagonally shorted coupled lines (a) and its equivalent circuit (b)

Fig. 2.3 Equivalent circuit of Hirota's reduced-size transmission line including artificial resonance circuits

Fig. 2.4 Final diagonally shorted miniaturized coupled lines with lumped capacitors equivalent to quarter-wave transmission line

Fig. 2.5 Equivalent lumped circuit of the quarter-wavelength transmission line

Fig. 2.6 Equivalent circuit of a quarter-wavelength transmission line with artificial resonance circuits inserted

Fig. 2.7 Parallel end shorted coupled lines (a) and its equivalent circuit (b)

Fig. 2.8 Final parallel end shorted miniaturized coupled lines with lumped capacitors equivalent to quarter-wave transmission line

Fig. 2.9 The open stub equivalent to the lumped capacitor C .

Fig. 2.10 Block diagram of a symmetrical Marchand balun as two identical couplers

Fig. 2.11 New structure for miniaturized balun filter(2.5-2)

Fig. 2.12 Sketch of perfect output port matching and isolation balun with resistive network

Fig. 2.13 Sketch of resistive network

Fig. 3.1 ADS model of the final diagonally shorted miniaturized coupled lines with equivalent to quarter-wave transmission line (a) and its frequency response of S11, S21 (b) and phase response (c)

Fig. 3. 2 ADS model of the initial miniaturized filter using open-stubs (a) and its frequency response of S11, S21 (b) and phase response (c)

Fig 3. 3 ADS model of the initial balun filter using the open-stubs for harmonic suppression(a),and its frequency response of S11, S21 S31 and phase response (c)

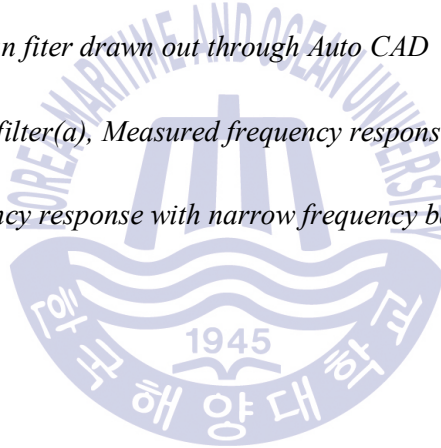
Fig 3. 4 Detailed value of coupled lines calculated by ADSLinecalc

Fig. 3.5 Layout of filter drawn by HFSS(a) frequency response(b) phase response (c)

Fig. 3.6 The circuit of balun filter drawn out through Auto CAD

Fig. 3.7 Fabricated balun filter(a), Measured frequency response(b), phase response(c)

Fig. 3. 8 Measured frequency response with narrow frequency bandwidth



Abstract

Recently, the area of radio frequency (RF) and microwave has been rapidly developed because it is widely used in wireless communication systems. The special function of RF front-end in the wireless communication transceiver makes it be the key and difficult in the research of wireless communication domain all around the world. In RF circuits, diagonally shorted and parallel end shored coupled lines of lumped capacitors which frequently can be used as RF basic components in many kinds of RF circuit such as balanced mixers, power amplifiers, and antenna feed networks. Thus, it is significant to reduce the size of transmission line and restrain harmonic to make RF bandpass filter (BPF) systems compact and implement easily. High performance is also needed while we seek the compact size. There are many problems in the some compact transmission filter, such as poor balanced port matching, which will limit their application.

In wireless applications, baluns which frequently connect a bandpass filter with a balanced component are significant system factors but usually occupy much of the volume of the systems. Thus, with the speedy development of modern communication, reducing the size of balun is the main challenge in making RF systems compact. In this paper, a new size-reduction method of balun filter using coupled lines with open-stub is presented. The characteristic of the new design was simulated on ADS and HFSS before fabricated on the FR4 epoxy glass cloth copper-clad plat (CCL) PCB substrate at center frequency of 0.88 GHz.

The theory and method related are fully explained in this paper. An extremely miniaturized transmission line filter based on diagonally shorted coupled lines of lumped capacitors which consisted of 18.7 degree coupled lines and operating at center frequency 0.88GHz has been fabricated on PCB substrate. The insertion loss of the balun filter is -3dB . The size of the overall circuit is $30\text{ mm} \times 16\text{mm}$.

Measurements results consisted with the simulated ones in acceptable sense. And theoretical, simulated and measured results are all demonstrated in the paper. The final experimental verification confirms the practicality and advantages of the proposed transmission line filter, etc.

KEY WORDS: miniaturization, coupled lines, isolation balun, bandpass filter, open-stub , harmonic suppression



CHAPTER 1 Introduction

1.1 RF filter introduction and basic parameters

There are many types of filter and can be divided into many kinds. Filters include low-pass filter, high-pass filter, band-pass filter, and band-stop filter according to frequency band; In terms of the frequency characteristic of insertion attenuation, there are bartwatts (smooth) filter, chebyshev filter and elliptic function filter; According to bandwidth, there are the narrow-band filter, medium-band filter and broadband filter, etc[1].

RF/Microwave filter has become a very important RF/Microwave components. For the low-frequency radio frequency signals, such as below 500 MHZ, lumped components may be used for the design of filter circuit. But the circuit parasitic parameters cannot be ignored when the RF signal at high frequency, the distributed parameter circuit is used to implement filtering circuit causing by the circuit parasitic parameters cannot be ignored[2]. The distribution parameters of the filter are mainly implement through transmission line. According to the transmission line type to points, filters can be divided into waveguide filter, coaxial line and microstrip line, stripline filter filter filter, etc[3].

A large amount of filters is needed as the multi-frequency works are more and more common because of the increasing on corresponding to the requirement of space frequency increase. The application of microwave solid state devices also have a role to the development of filter, such as microwave solid doubler circuit components are more frequency work, needs the corresponding filter. At the same time, the electronic equipment to reduce volume, weight, has become an important problem that induces a development trend of microwave electronic devices to develop highly integrated and miniaturization[4]. Therefore, microstrip filter with the significant advantages of microstrip line is developing rapidly.

The main difference among Microstrip filter, waveguide and coaxial microwave filter lies in the form of transmission line. In terms of main characteristics, such as using a lumped parameter or distributed parameter structure is the same, so about some basic concepts of microwave filter and the basic design method of microstrip filter applies [4].

There are two kinds of method to analysis and design Microwave/RF filter named distributed parameters and lumped parameters, respectively. And the lumped parameter can be divided into two small classes, imaging method and the network synthesis, respectively[5]. Distributed parameter method is inserted according to insertion attenuation and phase shift function, finding the microwave filter element structure under application of the theory of transmission line or waveguide directly. Imaging method based on image parameter can get the equivalent circuit of the low frequency network theory to design each component using microwave structure to simulate. Network synthesis is based on the attenuation and phase shift function, using the theory of network synthesis, first take the lumped element low-pass prototype circuit (using appropriate frequency transformation function, can transform for the need of low-pass, bandpass, band stop), then, then lumped elements, each element in the prototype circuit structure with microwave to achieve [5]. Distributed parameter method and the image parameter method calculation of the two methods of multifarious, degree of approximation is poor, and unable to export the best design, so now the design of microwave filters used more based on network synthesis method of lumped element low-pass prototype circuit, all kinds of low-pass, high-pass, band-pass, the transmission properties of band-stop filter are derived based on the prototype characteristics.

The prototype circuit aims to use inductor L , capacitance C as lumped parameters of low frequency circuit components. By using different integrated design methods, can obtain a series of normalized element values of capacitor C and inductor L values[6]. Usually, the prototype low-pass filter mainly includes Butterworth (flat) prototype filter, Chebyshev (corrugated) prototype filter and elliptic

function prototype filter. The first step for integrated design prototype low-pass filter, is to determine the order of filter through insert attenuation characteristics and out-of-band attenuation performance requirements. The network structure of prototype low-pass filter is determined while the order is determined. And the parameters of the prototype low-pass filter can be achieved through the look-up table. According to certain transformation of the low-pass filter design, translate the low-pass prototype based on a certain transformation relationship circuit component parameters into actual component values of the filter when making a specific filter design. Then convert lumped components to the distribution parameters, the actual RF distribution parameters filter is designed.

In this thesis, a novel extremely ease processed filter is designed using open-stub equivalent circuit to replace capacitor based on diagonally and parallel shorted miniaturized coupled lines. Using diagonally and parallel shorted miniaturized coupled lines can largely reduce the electrical length of transmission lines while maintaining acceptable characteristic around the center frequency. The method of using open-stub can make the circuit in a plane to achieve and can be easily realized on printed circuit board(PCB). Theoretical analysis and design formulas are derived. To demonstrate the feasibility and validity of the design equations, experimental verification of such a compact transmission filter working at 0.88MHz is presented. It is simulated by Agilent ADS and HFSS and implemented on printed circuit board (PCB). The fabricated transmission filter has a small area of 30mm×16mm, not including the extended space for testing, a wider upper stopband and phase difference of 182 degree at the two balanced ports over the operating frequency band. The measurement results agree well with the simulation, which demonstrates that the proposed filter has great application potential.

1.2 Background and Introduction of Balun

Balun are key components in many wireless and mobile communication

systems as well as microwave, millimeter-wave and RF circuits such as double balanced mixers[7][8], push-pull amplifiers[9], frequency doublers[10], multipliers and antenna excitations in order to reduce the noise and higher-order harmonics and improve the dynamic range of the systems. Functionally, a balun is a device intended to act as a transformer, matching an unbalanced circuit to a balanced one, or vice versa, with minimum loss and equal balanced impedances. The signal of a balanced circuit structure comprises two signal components with the same magnitude but 180 phase difference [11] [12]. There are several types of baluns that are either active or passive. The major advantage of active baluns is the small size, which makes them suitable to integrate into ICs. However, the performances of active baluns including linearity, noise figure, and balance property are usually not satisfactory as well as exhaust more energy [13]. Passive baluns can be classified as lumped-type [14], coil-type [15], and distributed-type baluns [12]. The advantages of a lumped-type balun are small volume and light weight. However, it is not easy to maintain 180 phase difference and identical magnitude between the two signals. Coil-type baluns have been widely used in lower frequency and ultra high frequency (UHF) bands. When a coil-type balun is used in higher than the UHF band, it usually has a drawback of having considerable loss. Distributed-type baluns can further be classified as a 180 hybrid balun and a Marchand balun. A 180 hybrid balun has a fairly good frequency response in the microwave frequency band. However, its size often poses a problem when it is used in the radio frequency range between 200 MHz and several GHz.

Among the various kinds of baluns, a planar version of Marchand balun, illustrated in Fig. 1.1, has been adopted for a long time due to its planar structure, good amplitude, phase balance characteristics and inherently wide operation bandwidth. Both phase difference and power distribution of a Marchand balun are reasonably good. A Marchand balun is commonly used in the industry comprises two sections of quarter-wave coupled lines [16] which may be realized using parallel-coupled microstrip lines [17], Lange couplers [18], multilayer coupled structures [19], or spiral coils [13]. Nevertheless, the Marchand balun consisting of

two identical $\lambda/4$ coupled lines still occupies a big area, especially at low frequencies.

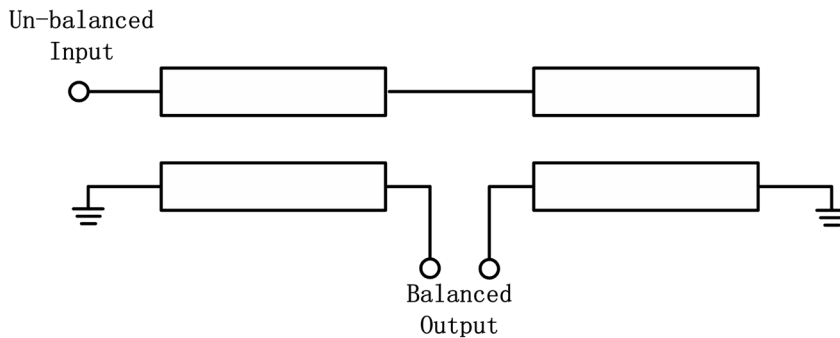


Fig. 1.1 A planar version of Marchand balun

The first transmission line balun was described in the literature by Lindenblad [20] in 1939 and variations on his original scheme soon followed. Among these was that of Marchand, who introduced a series open-circuited line to compensate for the short circuited line reactance of the two wires. Three other variations were cataloged and described by the Harvard Radio Research Laboratory staff [21]. Harvard's Type II balun is similar to Marchand's variation but without compensation. Because of the compensating feature of Marchand's variation, the author suggests the name "compensated balun" to distinguish it from the others. In 1957, Roberts [22] apparently reinvented the compensated balun and the author used Roberts' paper as a starting point of his initial analysis [23]. In 1958, McLaughlin, Dunn, and Grow [24], using Marchand's paper, designed a 13-to-1 bandwidth compensated balun which is the broadest thus far published. Bawer and Wolfe [25] subsequently applied the compensated balun to a broadband spiral antenna.

In design of a coupled-line Marchand balun, various analysis methods were presented. They are usually designed through circuit simulations using full-wave electromagnetic analysis [7] or lumped-element models [14]. Various synthesis techniques using coupled-line equivalent-circuit models and analytically derived scattering parameters have also been reported [26]. In [8], use of the relationships of

the power wave in a balun to derive the scattering parameters can analyze a symmetrical Marchand balun, but the exact prediction is only valid at the center frequency. In [27], inclusion of the parameter of the electrical length of the transmission line can predict broadband performances, but the approach lacks generality. Furthermore, to achieve wider bandwidth, multiconductor coupled lines to realize tight couplings were presented. Another method is the even- and odd-mode analysis method. However, it is limited to the case of a symmetrical coupled-line Marchand balun with the maximally flat responses.

In addition, most of the work on improving the planar Marchand balun has focused on achieving wide-band performance and miniaturization. The issue of balun output matching and isolation has not been addressed. This may be attributed to the well-known fact that a lossless reciprocal three-port network such as the balun cannot achieve perfect matching at all three ports. In many applications, however, balun output matching and isolation can enhance circuit performance. In double-balanced diode mixers, good output matching of the local oscillator (LO) and RF baluns at the diode interfaces can reduce LO power drive requirements and improve conversion loss. In push-pull amplifiers, isolation between the transistors provided by the balun outputs can enhance amplifier stability. In [28], a resistive network connected between the balun outputs is proposed to achieve balun output matching and isolation. Combining this technique with impedance transforming Marchand baluns, a class of perfectly matched impedance-transforming baluns can be realized. Whereas, this bulky resistive network consumes a large circuit area.

In some wireless applications, especially for WLAN and Bluetooth systems, the balun frequently connects a bandpass filter (BPF) with a balanced component, such as low noise amplifier (LNA), monolithic microwave integrated circuit (MMIC). Hence an integration of a BPF and a balun is necessary to reduce the cost and the size of the functional block in the systems. Recently, to meet the need, a balanced filter has been reported. However, the balanced filter, simply, uses an integration concept of the two components using an inter-matching circuit and,

hence, the resultant filter is a very complicated component.

In this thesis, a novel balun filter for size extremely miniaturization is demonstrated utilizing the combination of diagonally shorted coupled lines and parallel end shorted coupled lines. The method of adding open-stub acting as lumped capacitors to the conventional coupled line section can largely reduce the required electrical length of coupled line while maintaining approximately the same characteristic around the center frequency and effectively suppress the spurious passband. Furthermore, by employing an improved the value of capacitors and the size of open-stubs, the perfect balanced ports matching and isolation can be achieved. Theoretical analysis and design formulas are derived. To prove the feasibility and validity of the design equation, experimental verification of such a compact balun filter working at 0.88MHz is presented. It is simulated by ADS and HFSS and implemented on printed circuit board (PCB). The fabricated balun filter has a small area of 32mm×17mm, not including the extended space for testing, a wider upper stopband and phase difference of 180 degree at the two balanced ports over the operating frequency band. The measurement results agree well with the simulation, which demonstrates that the proposed filter has great application potential.

1.3 Organization of the Thesis

The contents of the thesis are illustrated as follows:

Chapter 1 briefly introduces the background, purpose and outline of this work.

Chapter 2 describes the size-reduction method for quarter-wave transmission line by using parallel and diagonally end shorted coupled lines both with shunt lumped capacitors. After that, the open-stub circuit method is introduced. Then it

presents the design procedure of such a new configuration filter based on quarter-wave transmission line.

Chapter 3 displays the simulated results by ADS and HFSS and the experimental and measured results of fabricated balun filter.

Chapter 4 gives the conclusion of this work.



CHAPTER 2 Balun Filter Design Theory

The conventional parallel coupled lines are useful and widely applied structures that provide the basis for many types of components, including directional couplers, power splitters and combiners, duplexers, filters, phase shifters, transformers and the aforementioned baluns. The microstrip parallel coupled filter is first proposed by Cohn in 1958 [29]. This type of filter is popular because of its planar structure, insensitivity to fabrication tolerance, wide realizable bandwidth [30]–[32], and simple synthesis procedures [33]. However, despite its advantages, the traditional parallel coupled-line filter has several shortcomings. One of the disadvantages is that it suffers from spurious responses that are generated at the multiples of operating frequency due to the unequal even- and odd-mode phase velocities of the coupled line. The stopband rejection performance is thus severely degraded. Another is the whole length of the filter is too long. Both disadvantages greatly limit the application of this type of filter. To overcome these problems, the size reduction methods are introduced in this chapter.

2.1 Size Reduction Method

As is well known, the quarter-wavelength transmission line has been playing a very important role in many microwave circuits. However, in many cases, it is too large to be compatible with other parts of microwave systems. The size reduction method proposing by Hirota [34] is attractive in view of using lumped capacitors and short transmission line. But the circuit size could not be much reduced due to the limitation of the high impedance of the transmission line.

2.1.1 Diagonally Shorted Coupled Lines with Lumped Capacitors

The reduced quarter-wavelength transmission line using combination of shorted transmission line and shunt lumped capacitors proposed by Hirota is shown in Fig. 2.1.

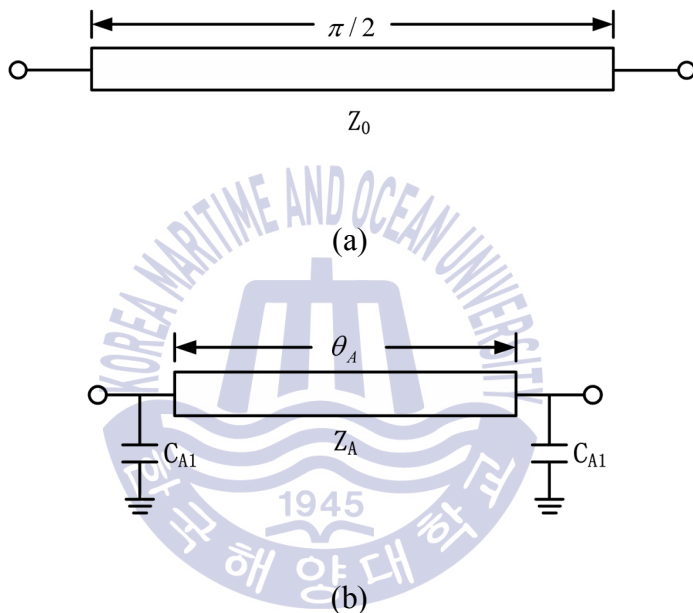


Fig. 2.1 Quarter-wave transmission line (a) and its equivalent shorted transmission line circuit (b)

The relations between the quarter-wavelength line and the reduced line can be estimated using ABCD matrices.

$$\begin{bmatrix} A & B \\ C & D \end{bmatrix}_{\left(\frac{\lambda}{4}, Z_c\right)} = \begin{bmatrix} \cos\theta & jZ_c \sin\theta \\ j\frac{1}{Z_c} \sin\theta & \cos\theta \end{bmatrix} = \begin{bmatrix} 0 & jZ_c \\ j\frac{1}{Z_c} & 0 \end{bmatrix} \quad (2.1-1)$$

$$\begin{aligned}
 \begin{bmatrix} A & B \\ C & D \end{bmatrix}_{(equivalent)} &= \begin{bmatrix} 1 & 0 \\ j\omega C_{A1} & 1 \end{bmatrix} \begin{bmatrix} \cos\theta_A & jZ_A \sin\theta_A \\ \frac{j}{Z_A} \sin\theta_A & \cos\theta_A \end{bmatrix} \begin{bmatrix} 1 & 0 \\ j\omega C_{A1} & 1 \end{bmatrix} \\
 &= \begin{bmatrix} \cos\theta_A - \omega C_{A1} Z_A \sin\theta_A & jZ_A \sin\theta_A \\ j(2\omega C_{A1} \cos\theta_A + Y_1 \sin\theta_A - \omega C_{A1} Z_A \sin\theta_A) & \cos\theta_A - \omega C_{A1} Z_A \sin\theta_A \end{bmatrix} \quad (2.1-2)
 \end{aligned}$$

By equating ABCD matrices of (2.1-1) and (2.1-2), equations for calculating values of Z_A and C_{A1} are derived.

Then we can get the related equations are as follows,

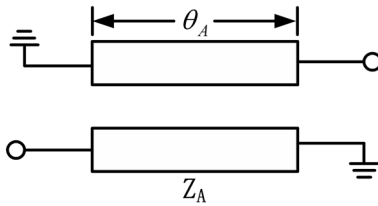
$$Z_A = \frac{Z_0}{\sin\theta_{A1}} \quad (2.1-3)$$

$$\omega C_{A1} = \frac{\cos\theta_{A1}}{Z_0} \quad (2.1-4)$$

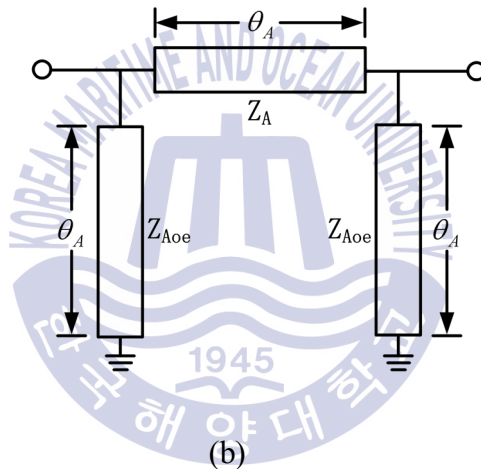
where Z_A , Z_0 , θ_A and ω are the characteristic impedance of the shorted transmission line, the characteristic impedance of the quarter-wavelength line, the electrical length of the shorted line and angular frequency, respectively.

From (2.1-3), it is clear that the characteristic impedance of the shorted transmission line Z_A goes higher as the electrical length θ goes smaller. When it is highly miniaturized, the impedance Z_A will too high to obtain. In order to reach very small electrical length up to several degrees, the coupled line component was adopted.

Fig.2.2 (a) and (b) show the diagonally shorted coupled lines and its equivalent circuit[35]



(a)



(b)

Fig. 2.2 Diagonally shorted coupled lines (a) and its equivalent circuit (b)

The characteristic impedance of the diagonally shorted coupled lines can be represented by the even-mode and odd-mode characteristic impedance and thus is given by:

$$Z_A = \frac{2Z_{Aoe}Z_{Aoo}}{Z_{Aoe} - Z_{Aoo}} \quad (2.1-5)$$

In Fig. 2.3, the artificial resonance circuits are inserted to Hirota's lumped distributed transmission line. Compare the dotted box part in Fig. 2.3 and the

equivalent circuit of the coupled lines in Fig. 2.2 (b). If the following equation is satisfied, the dotted box part in Fig. 2.3 can be replaced by the coupled lines [36].

$$\omega C_{A0} = \frac{1}{\omega L_{A0}} = \frac{1}{Z_{Aoe} \tan \theta_A} \quad (2.1-6)$$

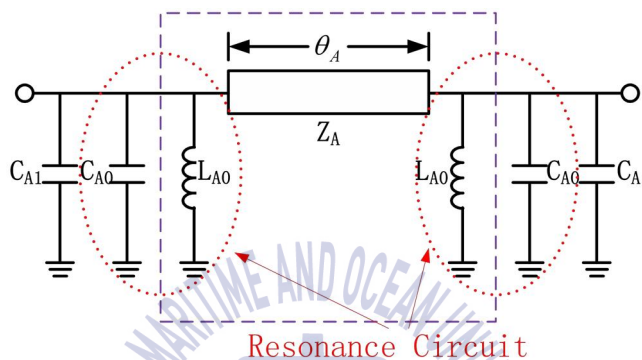


Fig. 2.3 Equivalent circuit of Hirota's reduced-size transmission line including artificial resonance circuits

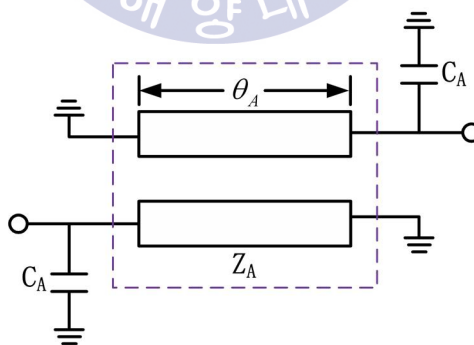


Fig. 2.4 Final diagonally shorted miniaturized coupled lines with lumped capacitors equivalent to quarter-wave transmission line

Finally, the two capacitors in each side of the Fig. 2.3 can combine mathematically. The structure of the diagonally miniaturized coupled lines with lumped capacitors appears as shown in Fig 2.4.

$$C_A = C_{A0} + C_{A1} = \frac{1}{\omega Z_{Aoe} \tan \theta_A} + \frac{\cos \theta_A}{\omega Z_0} \quad (2.1-7)$$

2.1.2 Parallel End Shorted Coupled Lines with Lumped Capacitors

As is well known, the quarter-wavelength transmission line also can be made equivalent to a lumped circuit, as given in Fig. 2.5, and the value of CB1 is given by

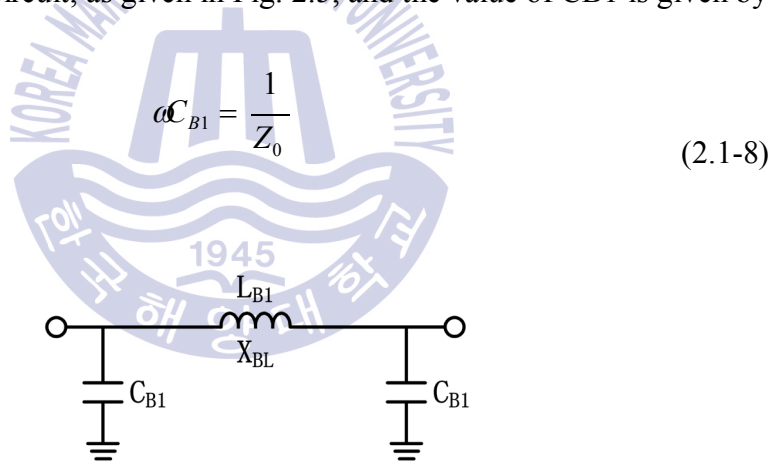
$$\omega C_{B1} = \frac{1}{Z_0} \quad (2.1-8)$$


Fig. 2.5 Equivalent lumped circuit of the quarter-wavelength transmission line

In order to replace the lumped inductor, firstly, the artificial resonance circuits are inserted to the circuit again at each side of the lumped inductor, as illustrated in Fig. 2.6. Furthermore, the dotted network can be made equivalent to the parallel end shorted coupled line section with electrical length of θ_B in Fig. 2.7 (a) and (b) when (2.1-9) and (2.1-10) are satisfied [35].

$$X_{B0} = Z_{Boe} \tan \theta_B \quad (2.1-9)$$

$$X_{BL} = \frac{2Z_{Boe} Z_{Boo}}{Z_{Boe} - Z_{Boo}} \tan \theta_B \quad (2.1-10)$$

where Z_{Boe} , Z_{Boo} are even- and odd-mode impedances of the parallel end shorted coupled line, respectively.

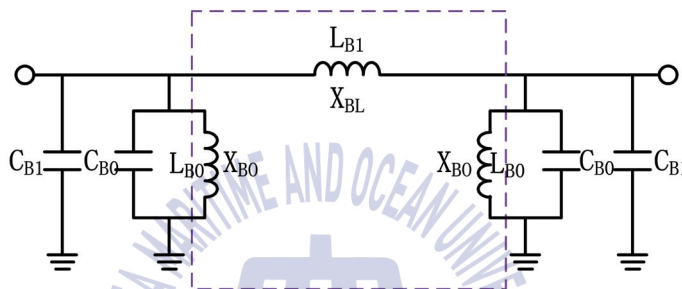
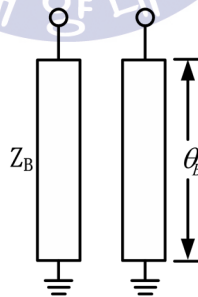


Fig. 2.6 Equivalent circuit of a quarter-wavelength transmission line with artificial resonance circuits inserted



(a)

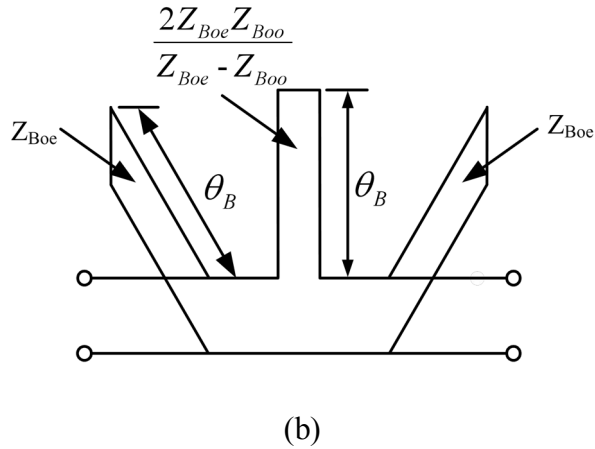


Fig. 2.7 Parallel end shorted coupled lines (a) and its equivalent circuit (b)

Fig. 2.8 is the schematic diagram of the initial miniaturized bandpass filter configuration and the value of the capacitors can be deduced from (2.1-9) as:

$$\omega C_{B0} = \frac{1}{Z_{Boe} \tan \theta_B} \quad (2.1-11)$$

$$C_B = C_{B0} + C_{B1} = \frac{1}{\omega Z_{Boe} \tan \theta_B} + \frac{1}{\omega Z_0} \quad (2.1-12)$$

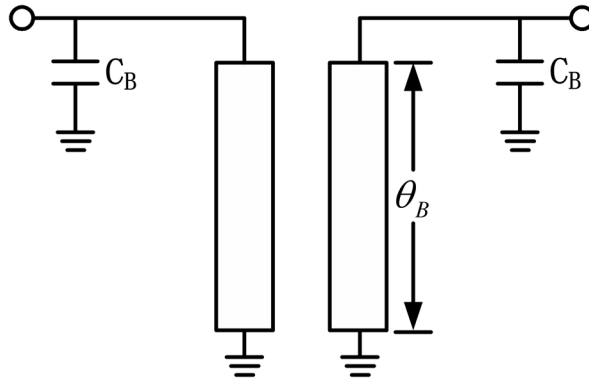


Fig. 2.8 Final parallel end shorted miniaturized coupled lines with lumped capacitors equivalent to quarter-wave transmission line

With (2.1-10), if defining the relationship between the characteristic impedance of the coupled-line and its even- and odd-mode impedances, we get:

$$Z_B = \frac{2Z_{Boe}Z_{Boo}}{Z_{Boe} - Z_{Boo}} = \frac{Z_0}{\tan\theta_B} \quad (2.1-13)$$

When the electrical length θ_B is very small for compact size, Z_B becomes very large. This large Z_B can be easily achieved by making Z_{Boe} and Z_{Boo} nearly the same.

2.2 The Open-stub Equivalent Circuit

The method of using open stub for n th harmonic suppression in modified Wilkinson power divider where n is the harmonic number is presented[37]. As shown in that paper, by placing a open stub at the center of each branch of the power divider and shunting the output ports with a parallel connection of a resistor and an inductor, the n th harmonic component and its odd multiples are suppressed without sacrificing the characteristics of the conventional Wilkinson power divider at the operating frequency. The T-type or π -type capacitive load flexible to the length is presented to suppress multiple harmonics[38]. This method also play a role

to reduce the generalized transmission line. By using T-type or π -type capacitive load equivalent to the quarter-wavelength transmission line, we can remove lumped inductor and the multiple harmonics can be suppressed.

In this paper, using a open stub at each side of the coupled line is presented to suppress multiple harmonics.

The open stub equivalent to capacitive load is shown in Fig.2.9.

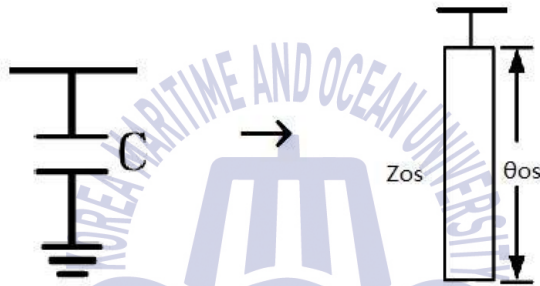


Fig. 2.9 The open stub equivalent to the lumped capacitor C.

In the case of open stub, the input impedance is expressed as follows,

$$Z_{in}(d) = -jZ_{os} \frac{1}{\tan(\beta d)} \quad (2.2-1)$$

When Z_{os} , d are the characteristic impedance and the length of the open stub, respectively. It would be equivalent to a capacitive behavior if the length of the open stub is less than quarter-wavelength of the transmission line.

$$Z_{in}(d) = -j \frac{1}{\omega C} \quad (2.2-2)$$

From (2.2-1),(2.2-2), we obtain

$$\omega C = \frac{\tan \theta}{Z_{os}} \quad (2.2-3)$$

$$Z_{os} = \frac{\tan \theta_{os} \cdot Z_A \sin \theta_A}{\cos \theta_A} \quad (2.2-4)$$

As we know, at the fundamental f_0 , the $\lambda/4$ open stub shorts the circuit and no transmission from the input to output ports. We use this fact to suppress harmonics by making the length of the open stub to $\lambda/4n$. In this case, at the n th harmonic frequency nf_0 , $\lambda/4n$ open stub shorts the circuit and make it more stable and easy to implement because of the ability of regulating the value of capacitance.

2.3 Ordinary Balun Design

Among the various kinds of baluns, a planar version of Marchand balun has been adopted for a long time due to its various advantages. This kind of balun has been well developed in [27]. A block diagram of the balun is shown in Fig. 2.10. It provides balanced outputs to load terminations Z_2 from an unbalanced input with source impedance Z_1 . In general, the impedances Z_1 and Z_2 are different. Thus, in addition to providing balanced outputs, the balun also needs to perform impedance transformation between the source and load impedances.

As shown in Fig. 2.10, the planar Marchand balun consists of two coupled sections, each of which is one quarter-wavelength long at the center frequency of operation. For symmetrical baluns, the scattering matrix of the balun can be derived from the scattering matrix of two identical couplers. We just consider the case where the source and load impedances are equal to Z_1 . The scattering matrix for ideal couplers with infinite directivity and coupling factor k is given by

$$[S]_{coupler} = \begin{bmatrix} 0 & k & -j\sqrt{1-k^2} & 0 \\ k & 0 & 0 & \sqrt{1-k^2} \\ -j\sqrt{1-k^2} & 0 & 0 & k \\ 0 & -j\sqrt{1-k^2} & k & 0 \end{bmatrix} \quad (2.4-1)$$

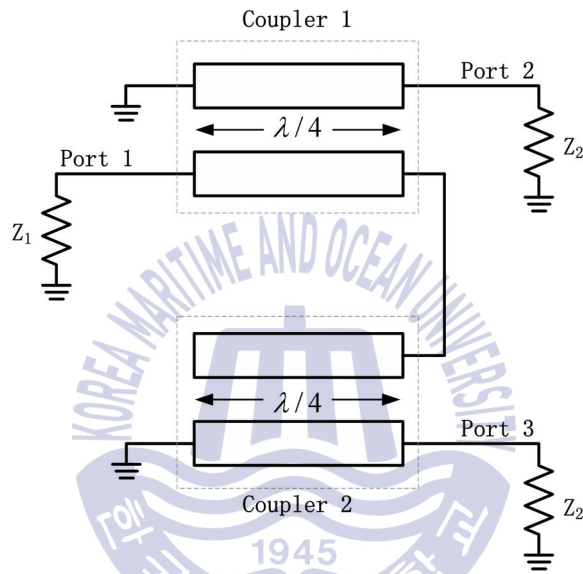


Fig. 2.10 Block diagram of a symmetrical Marchand balun as two identical couplers

The S-parameters of the balun can then be obtained, which has the form

$$[S]_{balun} = \begin{bmatrix} \frac{1-3k^2}{1+k^2} & j\frac{2k\sqrt{1-k^2}}{1+k^2} & \frac{2k\sqrt{1-k^2}}{1+k^2} \\ j\frac{2k\sqrt{1-k^2}}{1+k^2} & \frac{1-k^2}{1+k^2} & \frac{2k^2}{1+k^2} \\ -j\frac{2k\sqrt{1-k^2}}{1+k^2} & \frac{2k}{1+k^2} & \frac{1-k}{1+k^2} \end{bmatrix} \quad (2.4-2)$$

Equation (2.4-2) shows that the use of identical coupled sections results in balun outputs of equal amplitude and opposite phase, regardless of the coupling factor and port terminations. To achieve optimum power transfer of -3 dB to each port, we require

$$|S_{balun,21}| = |S_{balun,31}| = \frac{1}{\sqrt{2}} \quad (2.4-3)$$

With (2.4-2) and (2.4-3), the required coupling factor for optimum balun performance is given by

$$k = \frac{1}{\sqrt{3}} \quad (2.4-4)$$

When (2.4-4) is satisfied, the balun S matrix with parameters given by (2.4-2) reduces to

$$[S]^{balun} = \begin{bmatrix} 0 & \frac{j}{\sqrt{2}} & -\frac{j}{\sqrt{2}} \\ \frac{j}{\sqrt{2}} & \frac{1}{2} & \frac{1}{2} \\ -\frac{j}{\sqrt{2}} & \frac{1}{2} & \frac{1}{2} \end{bmatrix} \quad (2.4-5)$$

$$[Y]_{balun} = \begin{bmatrix} 0 & -\frac{jY_1}{\sqrt{2}} & \frac{jY_1}{\sqrt{2}} \\ -\frac{jY_1}{\sqrt{2}} & 0 & 0 \\ \frac{jY_1}{\sqrt{2}} & 0 & 0 \end{bmatrix} \quad (2.4-6)$$

2.4 New Structure for Miniaturized Balun Filter

Most of the work on improving the planar can achieve a perfect matching at the unbalanced port, but its poor balanced port matching and isolation limits its applications. For example, an extra output impedance-transforming matching network is needed for a push-pull amplifier design if a balun is applied at the power amplifiers' output.

First of all, because of the two kinds of miniaturized coupled lines provided in before, we can use these two section to achieve an extremely miniaturized balun filter. The corresponding Y parameters of two kinds of coupled lines expressed in Fig.2.11 in terms of the even and odd mode characteristic admittances Y_{oe} and Y_{oo} are given in [37]

$$[Y]_{couplerA} = \begin{bmatrix} Y_{A11} & Y_{A12} \\ Y_{A21} & Y_{A22} \end{bmatrix} = \begin{bmatrix} -j \frac{Y_{Aoo} + Y_{Aoe}}{2} \cot \theta_A & -j \frac{Y_{Aoo} - Y_{Aoe}}{2} \csc \theta_A \\ \frac{Y_{Aoo} - Y_{Aoe}}{2} & \frac{Y_{Aoo} + Y_{Aoe}}{2} \cot \theta_A \end{bmatrix} \quad (2.5-1)$$

$$[Y]_{couplerB} = \begin{bmatrix} Y_{B11} & Y_{B12} \\ Y_{B21} & Y_{B22} \end{bmatrix} = \begin{bmatrix} -j \frac{Y_{Boo} + Y_{Boe}}{2} \cot \theta_B & j \frac{Y_{Boo} - Y_{Boe}}{2} \cot \theta_B \\ \frac{Y_{Boo} - Y_{Boe}}{2} & \frac{Y_{Boo} + Y_{Boe}}{2} \cot \theta_B \end{bmatrix} \quad (2.5-2)$$

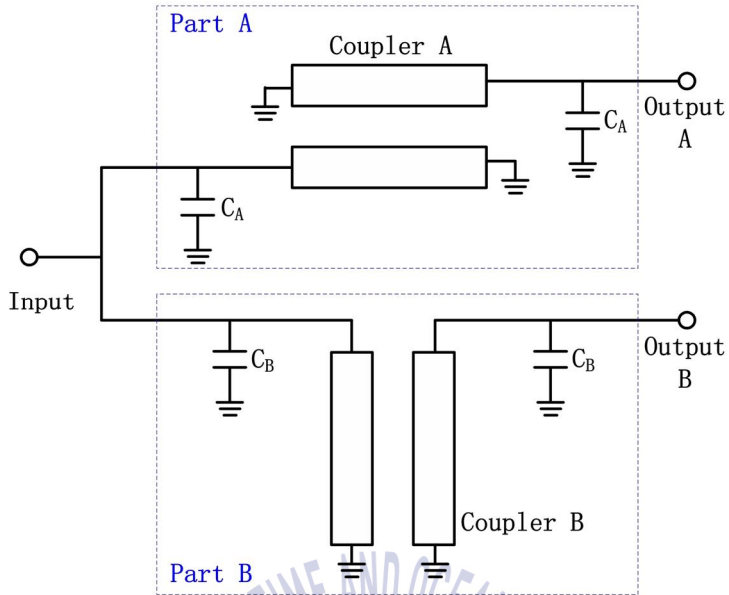


Fig. 2.11 New structure for miniaturized balun filter

After shunting the capacitors at each side of the coupled lines, the Y parameters of two parts are

$$[Y_A] = \begin{bmatrix} Y_{A11} & j\omega C_A \\ Y_{A21} & Y_{A12} + j\omega C_A \end{bmatrix} \quad (2.5-3)$$

$$[Y_B] = \begin{bmatrix} Y + j\omega C_B & Y \\ Y_{B12} + j\omega C_B & Y_{B22} \end{bmatrix} \quad (2.5-4)$$

As a series of relationship about the properties of two kinds of coupled lines are deduced above, every element of Y parameters in (2.5-3) and (2.5-4) can be worked out

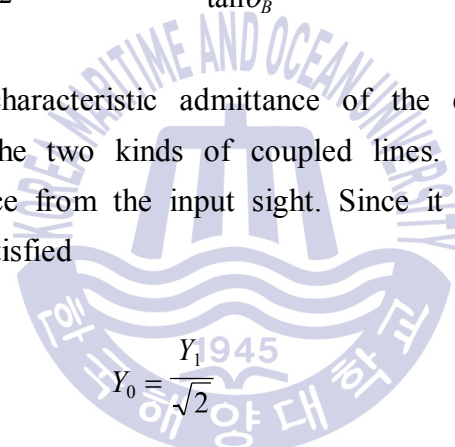
$$Y_{A11} + j\omega C_A = Y_{A22} + j\omega C_A = -j \frac{Y_{Aoo} + Y_{Aoe}}{2} \cot \theta + j \left(\frac{1}{Z_{Aoe} \tan \theta_A} + \frac{\cos \theta_A}{Z_0} \right) = 0 \quad (2.5-5)$$

$$Y_{A12} = Y_{A21} = -j \frac{Y_{Aoo} - Y_{Aoe}}{2} \csc \theta_A = -j \frac{Y_A}{\sin \theta_A} = -jY_0 \quad (2.5-6)$$

$$\begin{aligned} Y_{B11} + j\omega C_B &= Y_{B22} + j\omega C_B = -j \frac{Y_{Boo} + Y_{Boe}}{2} \cot \theta_B + j \left(\frac{1}{Z_{Boe} \tan \theta_B} + \frac{1}{Z_0} \right) \\ &= j \left(-\frac{1}{2} Y_{Boo} \cot \theta_B - \frac{1}{2} Y_{Boe} \cot \theta_B + Y_{Boe} \cot \theta_B + \frac{1}{Z_0} \right) \\ &= j \left(-\frac{Y_{Boo} - Y_{Boe}}{2} \frac{1}{\tan \theta_B} + \frac{1}{Z_0} \right) = j \left(-\frac{1}{Z_B \tan \theta_B} + \frac{1}{Z_0} \right) = 0 \end{aligned} \quad (2.5-7)$$

$$Y_{B12} = Y_{B21} = j \frac{Y_{Boo} - Y_{Boe}}{2} \cot \theta_B = j \frac{Y_B}{\tan \theta_B} = jY_0 \quad (2.5-8)$$

here Y_0 is the characteristic admittance of the equivalent quarter-wave transmission line of the two kinds of coupled lines. Y_1 is assumed as the characteristic admittance from the input sight. Since it is a power splitter, the relationship below is satisfied



$$Y_0 = \frac{Y_1}{\sqrt{2}} \quad (2.5-9)$$

Thus, the Y parameters of the whole tri-port circuit can be derived

$$\begin{aligned} [Y] &= \begin{bmatrix} \frac{Y_{A11} + Y_{B11} \omega + j\omega C_A + j\omega C_B}{Y_{A21}} & Y_{A12} & Y_{B12} \\ Y_{B21} & Y_{A22} + j\omega C_A & 0 \\ 0 & 0 & Y_{B22} + j\omega C_B \end{bmatrix} \\ &= \begin{bmatrix} 0 & -jY_0 & jY_0 \\ -jY_0 & 0 & 0 \\ jY_0 & 0 & 0 \end{bmatrix} = \begin{bmatrix} 0 & -jY_1 & jY_1 \\ -jY_1 & \sqrt{2} & \sqrt{2} \\ \frac{\sqrt{2}}{j} & 0 & 0 \\ \frac{1}{\sqrt{2}} & 0 & 0 \end{bmatrix} \end{aligned} \quad (2.5-10)$$

Based on the port terminations defined in Fig. 2.11, (2.5-10) can be converted to the scattering parameter matrix

$$\begin{aligned}
 [S] &= ([Y] - [Y])([Y] + [Y])^{-1} \\
 [S] &= \begin{bmatrix} Y_1 - Y_{11} & -Y_{12} & -Y_{13} & Y_1 + Y_{11} & Y_{12} & Y_{13} \\ -Y_{21} & Y_1 - Y_{22} & -Y_{23} & Y_{21} & Y_1 + Y_{22} & Y_{23} \\ -Y_{31} & -Y_{32} & Y_1 - Y_{33} & Y_{31} & Y_{32} & Y_1 + Y_{33} \end{bmatrix}^{-1} \\
 &= \frac{1}{2Y_1^3} \begin{bmatrix} Y_1 & \frac{jY_1}{\sqrt{2}} & -\frac{jY_1}{\sqrt{2}} \\ \frac{jY_1}{\sqrt{2}} & Y_1 & 0 \\ -\frac{jY_1}{\sqrt{2}} & 0 & Y_1 \end{bmatrix} \begin{bmatrix} Y_1^2 & \frac{jY_1}{\sqrt{2}} & -\frac{jY_1}{\sqrt{2}} \\ \frac{jY_1}{\sqrt{2}} & \frac{3Y_1}{2} & \frac{Y_1}{3\sqrt{2}} \\ -\frac{jY_1}{\sqrt{2}} & \frac{Y_1}{2} & \frac{Y_1}{2} \end{bmatrix} = \begin{bmatrix} 0 & \frac{j}{\sqrt{2}} & \frac{j}{\sqrt{2}} \\ \frac{j}{\sqrt{2}} & \frac{1}{2} & \frac{1}{2} \\ \frac{j}{\sqrt{2}} & \frac{1}{2} & \frac{1}{2} \end{bmatrix} \quad (2.5-11)
 \end{aligned}$$

This is same with (2.4-5), the S matrix of the ordinary Marchand balun. It is the best attainable S parameter matrix of a lossless balun which is matched at the input ($S_{11}=0$) and has transmission coefficients of -3dB ($|S_{21}| = |S_{31}| = (1/2)^{1/2}$) with opposite phase. The outputs, however, are not matched or isolated. Both the output matching and isolation have a value of -6dB ($|S_{22}| = |S_{33}| = |S_{23}| = |S_{32}| = 1/2$).

To achieve perfect output port matching and isolation, some form of resistive network need to be added between the output ports which are drawn in Fig.2.12 just as in the Wilkinson power divider. Y parameters will be used to derive the required resistive network. The S parameters matrix of a balun with perfect output matching and isolation has the form

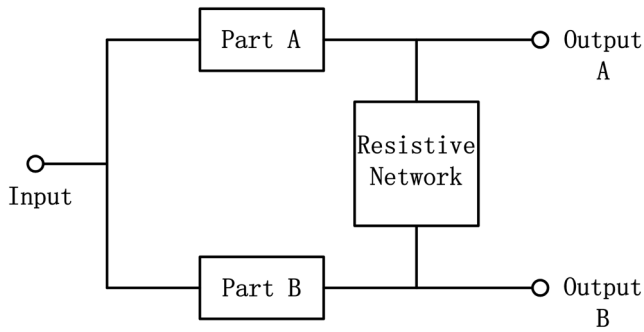


Fig. 2.12 Sketch of perfect output port matching and isolation balun with resistive network

$$[S]_{perfect} = \begin{bmatrix} 0 & j & -j \\ \frac{j}{\sqrt{2}} & \frac{1}{\sqrt{2}} & \frac{1}{\sqrt{2}} \\ \frac{-j}{\sqrt{2}} & \frac{1}{\sqrt{2}} & \frac{1}{\sqrt{2}} \end{bmatrix} \quad (2.5-12)$$

Similarly, the S matrix in (2.4-12) is converted to the Y matrix

$$[Y]_{perfect} = \begin{bmatrix} 0 & -jY_1 & jY_1 \\ -jY_1 & \frac{\sqrt{2}}{2}Y_1 & \frac{\sqrt{2}}{2}Y_1 \\ \frac{j}{\sqrt{2}}Y_1 & \frac{1}{2}Y_1 & \frac{1}{2}Y_1 \\ \frac{-j}{\sqrt{2}}Y_1 & \frac{1}{2}Y_1 & \frac{1}{2}Y_1 \end{bmatrix} \quad (2.5-13)$$

Comparing (2.4-11) and (2.4-12), it can be deduced that the Y matrix of the resistive network has the form

$$[Y]_R = \frac{1}{2Z_1} \begin{bmatrix} 1 & 1 \\ 1 & 1 \end{bmatrix} \quad (2.5-14)$$

$[Y_R]$ is the Y parameter matrix between 2 and 3 port of the novel balun. And where Y_1 is assumed as the characteristic admittance from the input sight. And then, compare the (2.5-6) and(2.5-13), there should be a network who's Y parameters matrix is (2.5-6) between port 2 and 3, like the Fig.2.12. $[Y_R]$ is the Y parameter matrix between 2 and 3 port of the novel balun.

Then we get the ABCD matrix from (2.5-6)

$$\begin{bmatrix} A & B \\ C & D \end{bmatrix} = \begin{bmatrix} -1 & -\frac{2}{Y_1} \\ 0 & -1 \end{bmatrix} = -1 \begin{bmatrix} 1 & \frac{2}{Y_1} \\ 0 & 1 \end{bmatrix} \quad (2.5-15)$$

In equation (2.5-15) we can see there is a -1 before the ABCD matrix, that means the resistance network is supposed to have a 180 degrees phase delay. And we also can conclude that the impedance of the resistance network value at $2/Y_1$, in other words is $2Z_1$. And the value Z_1 is 50Ohm.

So now we know the resistance network is supposed to have a phase inverter and series with resistor value at 100Ohm.

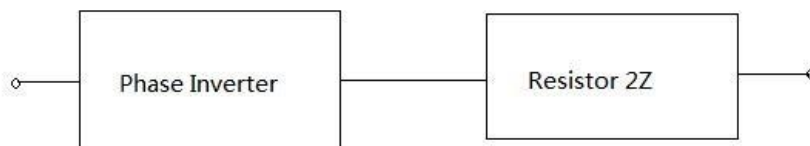


Fig. 2.13 Sketch of resistive network

But in this paper, the experiment only carried out until the design of combining two kinds of coupled line immediately causing by the short of time for my experiment.

CHAPTER 3 Simulation, Fabrication and Measurement

This chapter introduces the complete design procedure of a miniaturized bandpass filter including open stub with the specifications listed in Table 3.1 in greater detail based on the size reduction approach expatiated in last chapter to validate its availability. According to the above analysis, the coupled lines with short electronic length and high characteristic impedance are required for the miniaturized band-pass filter. To validate the analytical results and demonstrate the design approach in a time-efficient way, the circuit parameters are converted and simulated by circuit simulation software Agilent Advanced Design System (ADS) and full-wave 3-D EM simulation tool Ansoft HFSS. In order to simplifying the fabrication procedure as easy as can be realized in author's laboratory room, the circuit is implemented on printed circuit board (PCB).

Table 3.1 Ideal specifications of the proposed filter

Center frequency (GHz)	0.88 GHz
Fractional bandwidth (%)	13.75%
Insertion loss (dB)	-3.1 dB maximum
Stopband rejection (dB)	< -60 dB up to $10f_0$

3.1 Circuit Simulating by ADS and Analysis

We can confirm the theoretical values that calculated through the deduced equations through ADS simulation and obtain the width and length of each transmission line by ADS Line Calculation Tool. However, the ADS simulation and

calculation are carried out in ideal cases and have not taken many potential factors that may affect the performances of the band-pass filter into consideration. As its simulation speed is much faster than HFSS and the alteration tendency of the result can be observed easily while the circuit factors are tuning. So, simulation is carried out by ADS at the first step.

The initial miniaturized balun filter model illustrated in Fig. 2.11 with electrical length of coupled-line being 18.7° was obtained. When the even-mode impedance Z_{oe} was arbitrarily chosen as 79Ω , the value of the odd-mode impedance of the coupled-line Z_{oo} was 45Ω , making the coupling coefficient K being 0.274. The coupling coefficient K of the shorted coupled-line can determine the bandwidth of the proposed balun filter. The bandwidth increases as the coupling coefficient K does [34].

$$K = \frac{Z_{oe} - Z_{oo}}{Z_{oe} + Z_{oo}} \quad (3.1-1)$$

When the quarter-wavelength transmission line was miniaturized, one can choose a proper coupling coefficient according to the required bandwidth of the bandpass filter. However, to achieve a broad bandwidth, the coupling coefficient K should be made as large as possible, which means the difference between Z_{oe} and Z_{oo} should be large. It will result in a small characteristic impedance of the coupled lines and hence a large electrical length of them. Therefore, a necessary design trade-off between broad bandwidth and small circuit size should be considered.

With the obtained circuit parameters, the ADS model of the initial size-reduced balun filter was built as shown in below step by step and its frequency and phase response are also shown also from which we can observe the great agreement with our expectation.

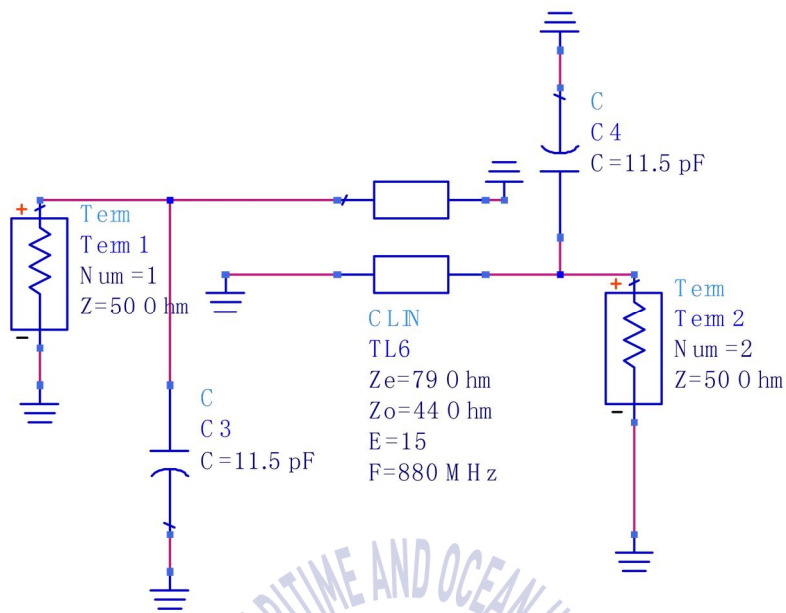
In many filter application, in order to reduce interference by keeping out-of-band signals from reaching a sensitive receiver, a wider upper stopband is

required. However, many planar filters which are comprised of half-wavelength resonators have an inherently spurious passband at 2ω , where ω is the center frequency. In this thesis, the proposed filter is reduced to just 18.8 degree using combinations of two kinds of coupled lines and open-stubs acting in capacitive. Therefore, the first spurious frequency can be shifted to much higher frequency for the electrical length of the resonant is very small.

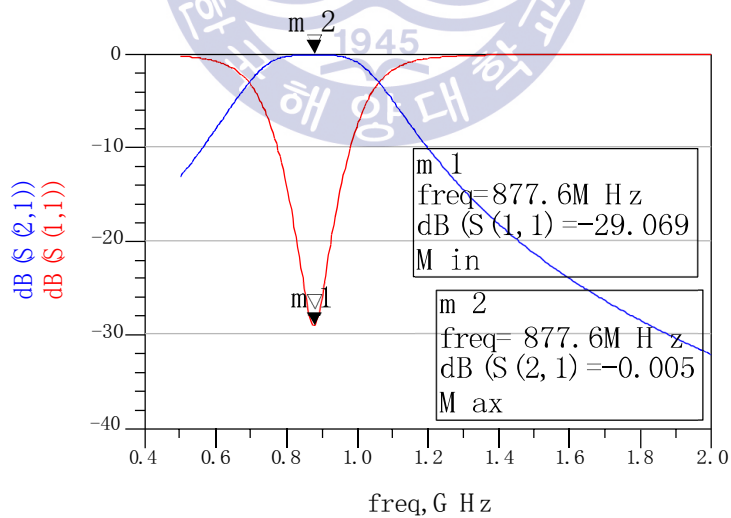
The broadband transmission characteristic of the ADS simulation result is illustrated in Fig. 3.2. It could be noted that there is no spurious response occurs for the frequency below 10GHz. In this case, the first spurious frequency is shifted to the position which is more than 10 times of the fundamental frequency.

3.1.1 Circuit Simulating of original coupled line circuit

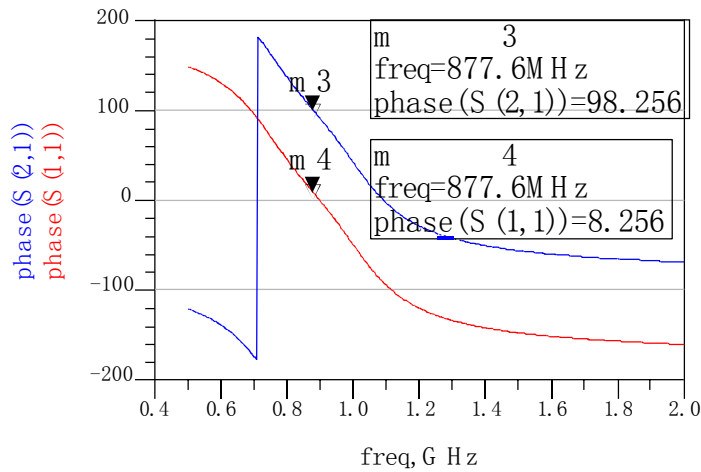
First step, using the Final diagonally shorted miniaturized coupled lines with lumped capacitors equivalent to quarter-wave transmission line to get a characteristic as filter. The ADS model of the circuit was built as given in Fig.3.1(a) and its frequency and phase response are also shown in Fig. 3.1 (b) and (c), respectively, from which we can observe the great agreement with our expectation.



(a)



(b)

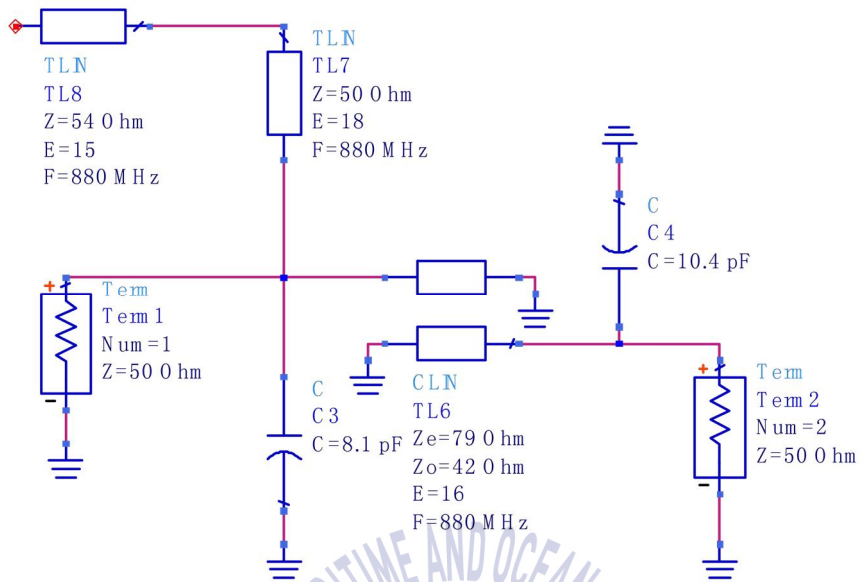


(c)

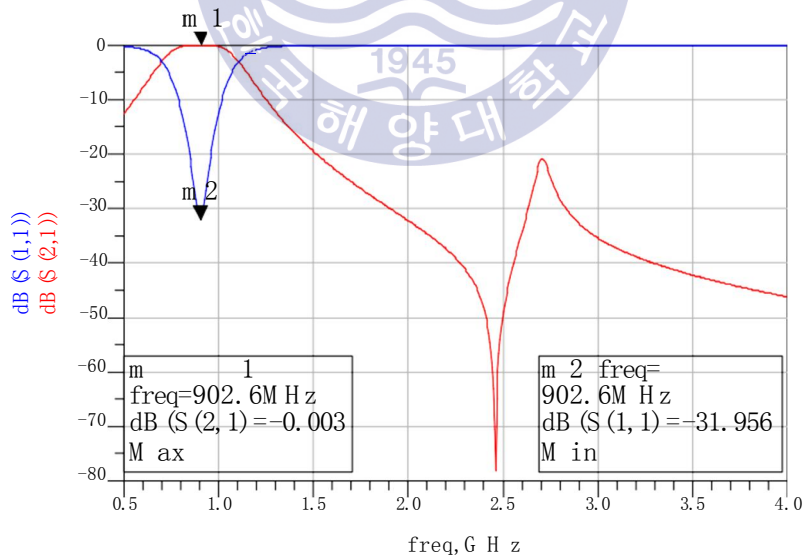
Fig. 3.1 ADS model of the final diagonally shorted miniaturized coupled lines with equivalent to quarter-wave transmission line (a) and its frequency response of S11, S21 (b) and phase response (c)

3.1.2 The equivalent Circuit Simulating by adding a open-stub to act in capacitive

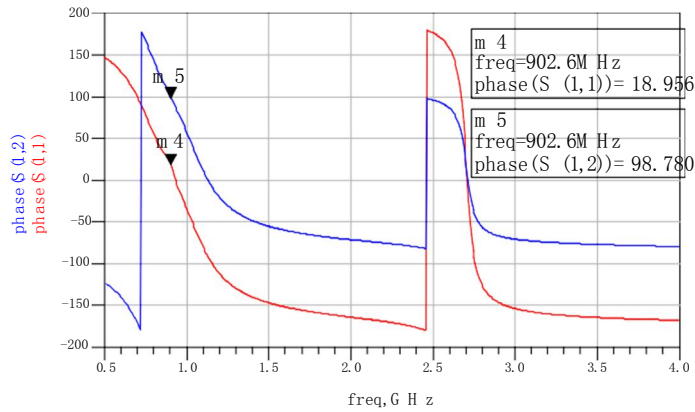
Using the open stub acting in capacitive at high frequency and divide it into two parts to make the size more reasonable. The ADS model of the circuit was built as given in Fig.3.2(a) and its frequency and phase response are also shown in Fig. 3.2 (b) and (c), respectively, from which we can observe the great agreement with our expectation.



(a)



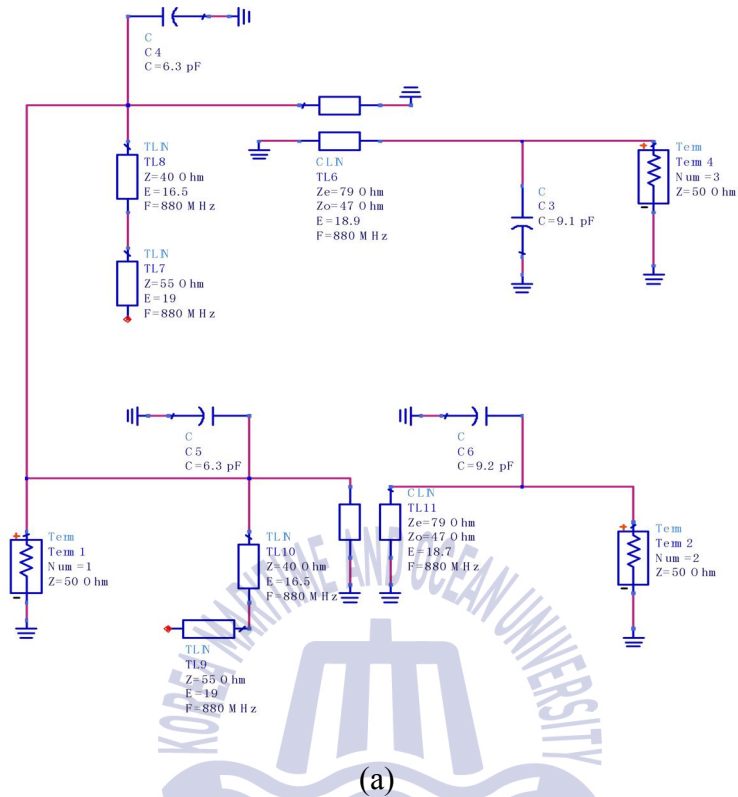
(b)



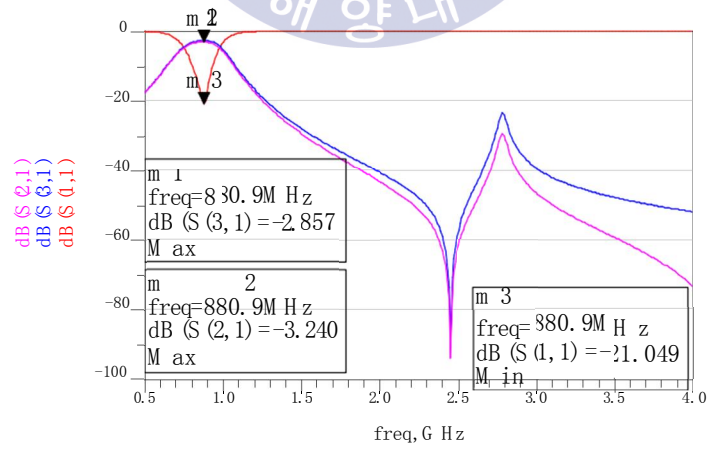
(c)

Fig. 3. 2 ADS model of the initial miniaturized filter using open-stubs (a) and its frequency response of S_{11} , S_{21} (b) and phase response (c)

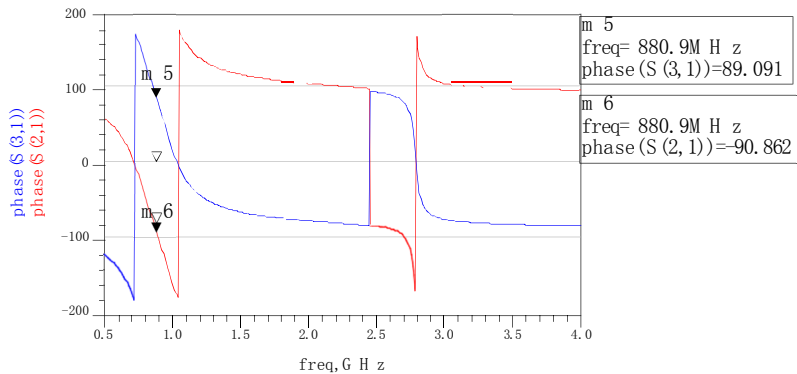
And then combine the two kinds of the coupled line circuit we can get the final ADS mode of the balun filter using open-stub for harmonic suppression as shown in Fig.3.3.



(a)



(b)



(c)

Fig 3. 3 ADS model of the initial balun filter using the open-stubs for harmonic suppression(a),and its frequency response of S11, S21 S31 and phase response (c)

3.2 Simulation by HFSS and Optimization

The theoretical values calculated through the deduced equations have been confirmed through ADS simulation. However, the ADS simulation and calculation are carried on in ideal cases, which have not taken many potential factors that may affect the performances of the coupler into consideration. At the same time two very sensitive composing parts of this coupler, capacitors and the connecting lines must be studied as they will be proved to be very sensitive in this designed circuit. For the above reasons, we used an electromagnetic simulator Ansoft HFSS to simulate the designed coupler before fabrication. On the other hand we can get to know the different parts that affect the performances of the whole circuit, and moreover we can save both the fabrication cost and time. The width and length of each transmission line can be obtained by ADS Line Calculation Tool, as given in Fig. 3.4.

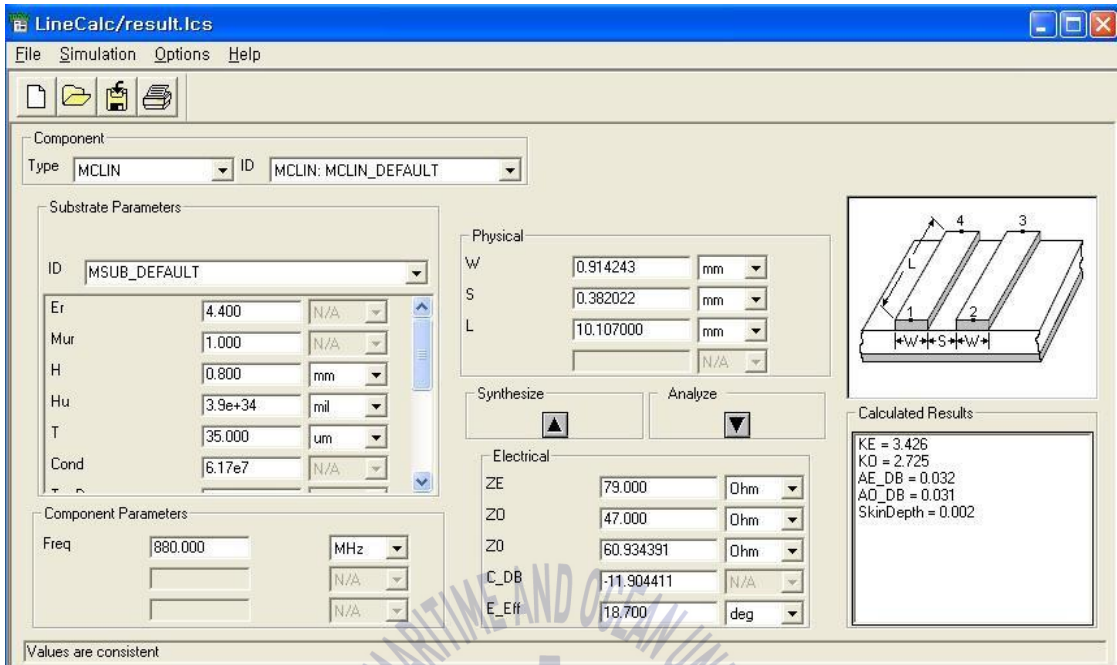


Fig 3. 4 Detailed value of coupled lines calculated by ADSLinecalc

Once the filter equivalent circuit model was built, physical filter structures such as resonators and coupled-line sections can be designed. However, one thing needs to be kept in mind that due to the parasitic components (both internally and externally) the synthesized filter model cannot be transformed into physical structures at one shot. As a result, some necessary tuning of the filter responses and optimizations of the filter physical dimensions should be carried out. Generally, it is carried out with Ansoft HFSS before fabrication until the full-wave electromagnetic (EM) simulation shows a good performance that close to the target one.

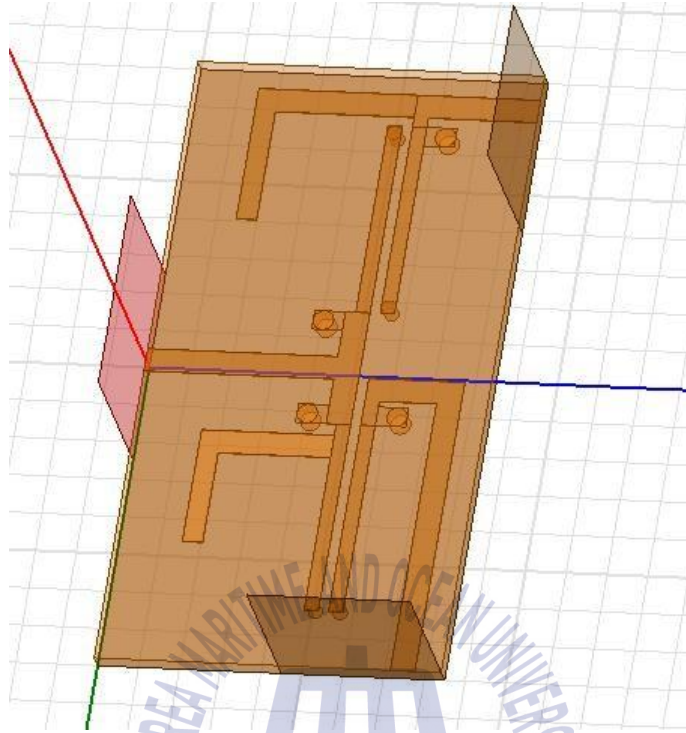
A transmission line filter working at 880MHz was designed to confirm the theories in the above chapters. Table 3.2 gives the design parameters of the HFSS simulation. Fig. 3.5 (a), (b) and (c) show the layout of the filter drawing in HFSS and its two kinds of simulation results, respectively.

Since considering the reciprocity between physical lines and optimizing the

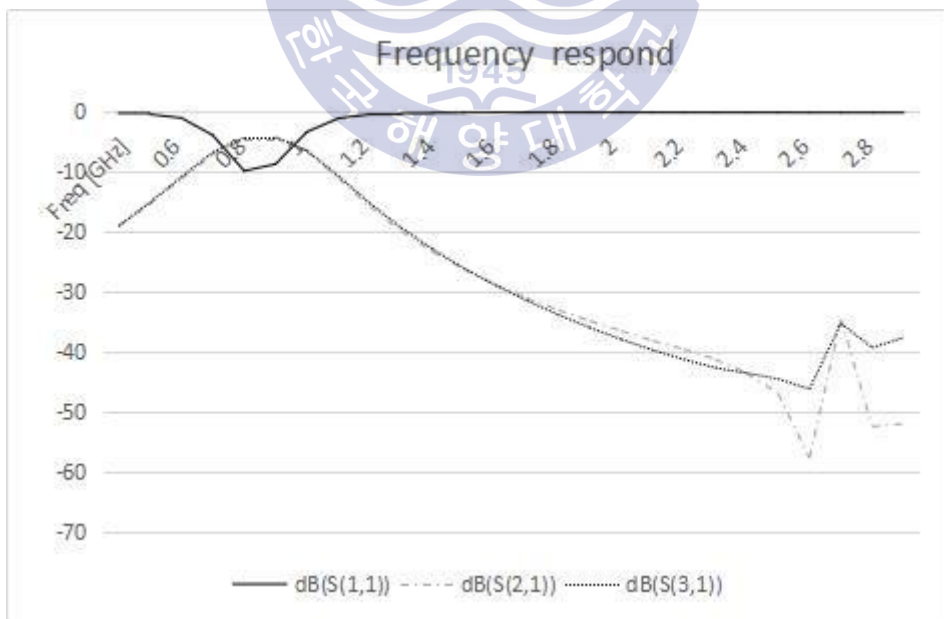
results to an expecting one. The values of the coupled lines element have been modified slightly. We can observe that final responses simulated by the full-wave simulator are almost the same as the responses optimized by the circuit simulator ADS. This proves the validity of this design method.

Table 3. 2 Design parameters of the HFSS simulation

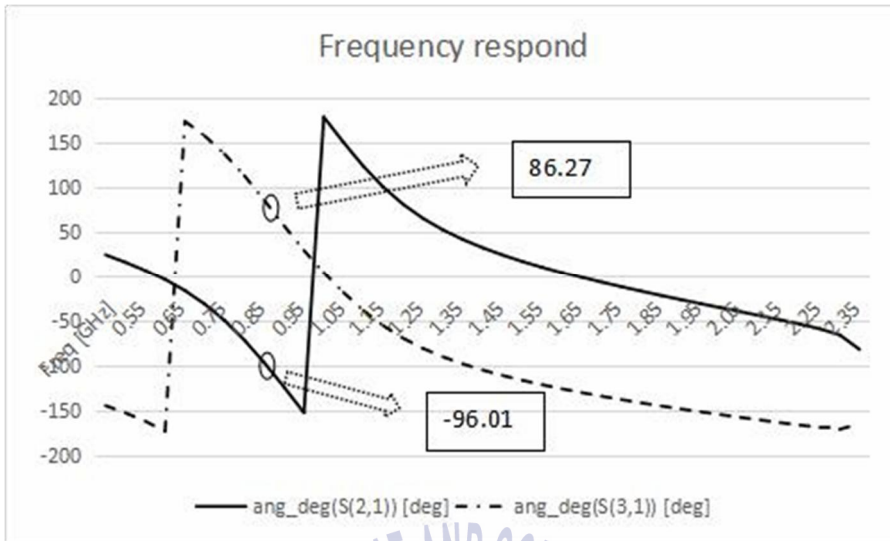
Center frequency	0.88GHz
Substrate thickness	0.8 mm
Substrate permittivity	4.4
Dielectric loss tangent	0.02
Copper thick ness	35 μ m
Copper cond uctivity	6.17 $\times 10^7$
Width of coupled lines	0.7mm
Length of coupled lines	10 mm
Slot of coupled lines	0.5 mm
Ports impedance	50 Ohm
Circuit size	30 mm \times 16mm



(a)



(b)



(c)

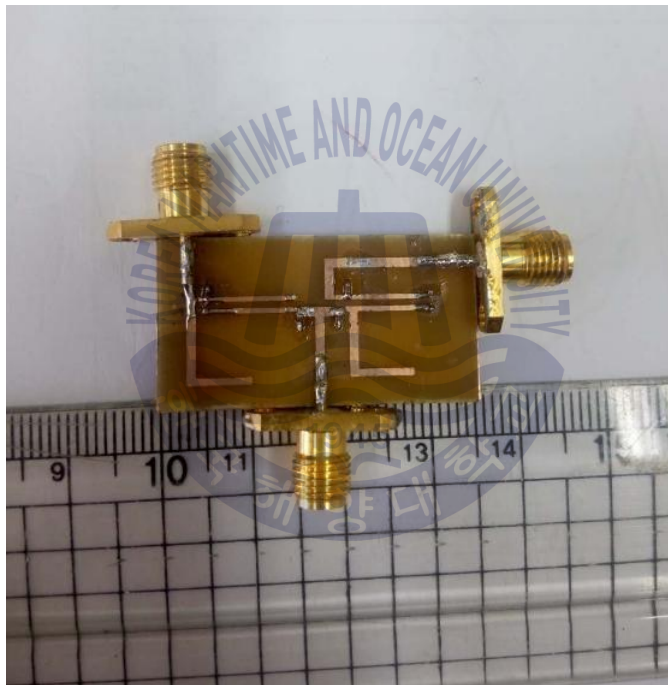
Fig. 3.5 Layout of filter drawn by HFSS(a) frequency response(b) phase response (c)

3.3 Fabrication and Measurement

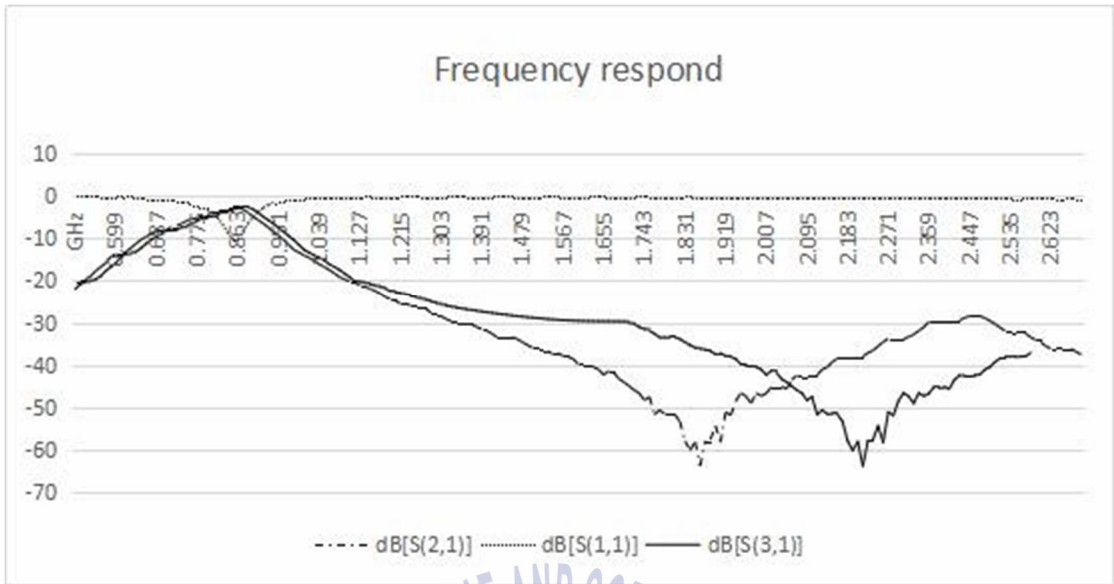
The layout of the filter used in fabrication which is drawn through Auto Computer Aided Design (AutoCAD) is given in Fig. 3.6, with the dimensions of the circuit area being 30mm×16mm. The filter is realized on the FR4 epoxy glass cloth copper-clad plat (CCL) PCB substrate having thickness 0.8mm and dielectric constant $\epsilon_r=4.4$. For the measurement convenience, all the balanced and unbalanced ports impedances are assumed to be 50Ohm. The photograph of the fabricated structure is displayed in Fig. 3.7.



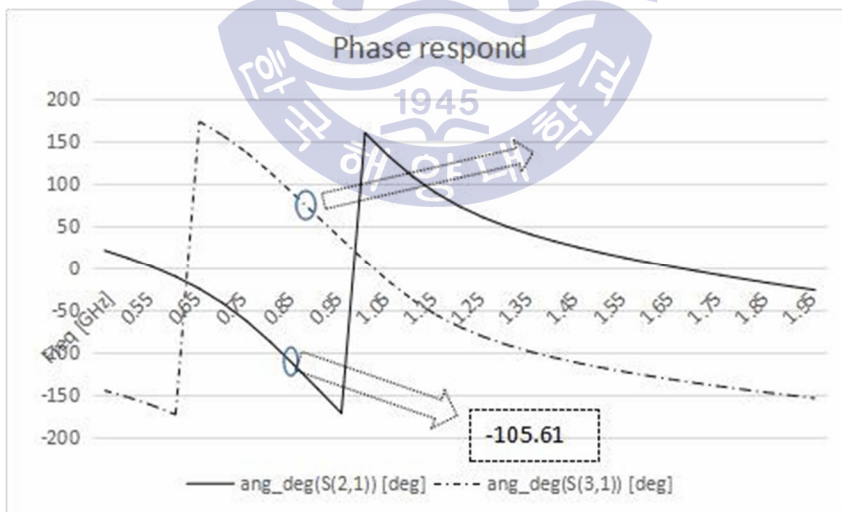
Fig. 3.6 The circuit of balun filter drawn out through Auto CAD



(a)



(b)



(c)

Fig. 3.7 Fabricated balun filter(a), Measured frequency response(b), phase response(c)

The figure of measurement frequency response with narrow frequency bandwidth, shown in Fig.3.8, which is much clear and distinguishable. So that it can

be ease to catch sight of the characteristic on the center frequency. Then we can get that the maximum of S_{21} and S_{31} are -4.2dB , -2.9dB at 872MHz and 886MHz , respectively. And there is phase delay about 186 degree at 880MHz between the two outputs. The inherently harmonic moves to 2.3GHz that around 2.6 . Both of the frequency and phase respond are basically satisfying with the simulation results.

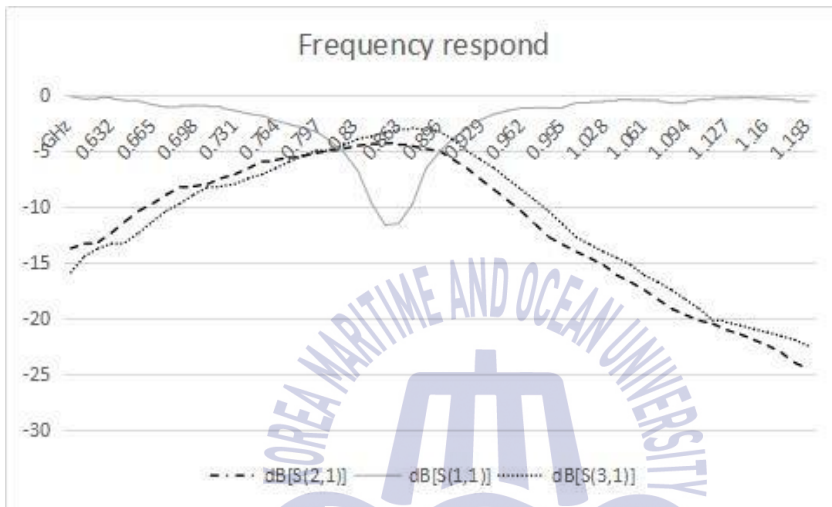


Fig. 3. 8 Measured frequency response with narrow frequency bandwidth

Chapter 4 Conclusion

In this thesis, we carry out the design theory and procedure for a novel balun filter extremely miniaturization utilizing diagonally and parallel end-shortened coupled lines with open-stubs for harmonic suppression. Shunt lumped capacitors can offer great amplitude and phase balance performance. It shows a wider upper stopband and broad bandwidth over the operating frequency. But when we adding a open-stub acting in capacitive, the amplitude might be not very good. The method of adding open-stubs to the conventional coupled line section can largely reduce the required electrical length and can make it in planar structure which can be ease realized by PCB. To demonstrate the feasibility and validity of the design equation, the size of 30mm×16mm, not including the extended space for testing, miniaturized balun filter is designed and fabricated on PCB substrate with the thickness of 0.8mm. The electrical length of the coupled lines is reduced to around 18 degree. According to the measurement results, it exhibits a bandwidth of 121MHz and 186 degree phase difference at the center frequency of 880MHz. The measurement responses basically agree with simulation result curves. This class of matched baluns is invaluable in the design of balanced microwave circuits that it makes this design suitable for microwave integrated circuit(MIC) and MMIC applications. It goes without saying that the theory of using open stub for harmonic suppression still requires a lot of research so as to gain more theoretical supports.

References

- [1] Ben-Bo Gan and X.C Wu, "The structure and design of modern filter", Science Press Co. Ltd.1973
- [2] W.Cheng, "The Research and design of microstrip ultra - broadband and multi-pass bandpass filters", Xidian University, 2012
- [3] S.Y EEr, "The Design and Production of LC Filter", Science Press Co.Ltd,Beijing,2006
- [4] H.Joshi, H.H Sigmarsson. M. Sungwook, D. Peroulis, and W.J. Chappell, "High Q Fully Reconfigurable Tunable Bandpass Filters", Microwave Theory and Techniques, IEEE Transactions on, vol,57,pp.3525-3533,2009
- [5] G.L.Matthaei. L. Young and E. Jones. Microwave Filter, Impedance-Matching Networks, and Coupling Structures. [M] McGraw-Hill New York,1964
- [6] S.B Cohn, Direct Coupled Cavity Filters for wide and narrow bandwidths, IEEE Trans on Microwave Theory and Techniques,1963,11(5): 162-178
- [7] T. Chen et al., "Broadband monolithic passive baluns and monolithic double balanced mixer", IEEE Trans. Microwave Theory Tech., vol. 39, pp.1980–1986, Dec. 1991.
- [8] S. C. Tseng, C. C. Meng, C. H. Chang, C. K. Wu and G. W. Huang, "Monolithic broadband Gilbert micromixer with an integrated Marchand balun using standard silicon IC process", IEEE Trans. Microwave Theory Tech., vol. 54, no. 12, pp. 4362–4371, Dec. 2006.
- [9] P. C. Hsu, C. Nguyen and M. Kintis, "Uniplanar broad-band push–pull FET amplifiers", IEEE Trans. Microwave Theory Tech., vol. 45, pp. 2150–2152, Dec. 1997.
- [10] S. A. Maas and Y. Ryu, "A broadband, planar, monolithic resistive frequency doubler", IEEE Int. Microwave Symp. Dig., pp. 443–446, 1994.
- [11] A. M. Pavio and A. Kikel, "A monolithic or hybrid broadband compensated balun", IEEE MTT-S Int. Dig., pp. 483–486 , 1990.
- [12] K. C. Gupta and C. Cho, "A new design procedure for single-layer and two-layer three-line baluns", IEEE Trans. Microwave Theory Tech., vol. 46, no. 12, pp. 2514–2519, Dec. 1998.
- [13] M. Rajashekharaiyah, P. Upadhyaya and H. Deukhyoun, "A compact 5.6 GHz low noise amplifier with new on-chip gain controllable active balun", in Proc. IEEE Workshop Microelectron Electron Devices, pp. 131–132, 2004.
- [14] Y. J. Yoon, Y. Lu, R. C. Frye, M. Y. Lau, P. R. Smith, L. Ahlquist and D. P. Kossives, "Design and characterization of multilayer spiral transmission- line baluns", IEEE Trans. Microwave Theory Tech., vol. 47, no. 9, pp. 1841–1847, Sep. 1999.
- [15] B. A. Munk, Balun, etc., 3rd ed, J. D. Kraus and R. J. Marhefka, Eds. New York: McGraw-Hill, ch. 23, 2002.

- [16] N. Marchand, "Transmission-Line Conversion Transformers", *Electronics*, vol. 17, pp. 142–146, Dec. 1944.
- [17] W. R. Brinlee, A. M. Pavio and K. R. Varian, "A novel planar double -balanced 6–18 GHz MMIC mixer", *IEEE Microwave Millimeter-Wave Monolithic Circuit Symp. Dig.*, pp. 139–142, 1994.
- [18] M. C. Tsai, "A new compact wide-band balun", *IEEE Microwave and Millimeter Wave Monolithic Circuit Symp. Dig.*, pp. 123–125, 1993.
- [19] K. Nishikawa, I. Toyoda and T. Tokumitsu, "Compact and broad-band three-dimensional MMIC balun". *IEEE Trans. Microwave Theory Tech.*, vol. 47, pp. 96–98, Jan. 1999.
- [20] N. E. Lindenblad, "Television transmitting antenna for Empire State Building ", *RCA Rev.*, vol. 3, pp. 387-408, Apr. 1939.
- [21] Radio Research Laboratory Staff, *Very High-Frequency Techniques*. New York: McGraw-Hill, vol. 1, p. 88, 1947.
- [22] W. K. Roberts, "A new wide-band balun", *Proc. IRE*, vol. 4.5, pp. 1628–1631, Dec. 1957.
- [23] H. G. Oltman, Jr., "Analysis of the compensated balun", *Rantec Corp., Calif., Tech. Rept.*, May 1961.
- [24] J. W. McLaughlin, D. A. Dunn, and R. W. Grow, "A wide-band balun", *IRE Trans. on Microwave Theory and Techniques*, vol. MTT- 6, pp. 314-316, July 1958.
- [25] R. Bawer and J. J. Wolfe, "A printed circuit balun for use with a spiral antenna", *IRE Trans. on Microwave Theory and Techniques*, vol. MTT-8, pp. 319–325, May 1960.
- [26] R. Schwindt and C. Nguyen, "Computer-aided analysis and design of a planar multilayer Marchand balun", *IEEE Trans. Microwave Theory Tech.*, vol. 42, pp. 1429–1434, July 1994.
- [27] C. S. Lin, P. S. Wu, M. C. Yeh, J. S. Fu, H. Y. Chang, K. Y. Lin, and H. Wang, "Analysis of multiconductor coupled-line Marchand baluns for miniature MMIC design", *IEEE Trans. Microw. Theory Tech.*, vol. 55, no. 6, pp. 1190–1199, Jun. 2007.
- [28] K. S. Ang and I. D. Robertson, "Analysis and design of impedance transforming Marchand balun", *IEEE Trans. Microwave Theory Tech.*, vol. 49, pp. 402–405, Feb. 2001.
- [29] S. B. Cohn, "Parallel-coupled transmission-line-resonator filters", *IRE Trans. Microw. Theory Tech.*, vol. MTT-6, no. 4, pp. 223–231, Apr. 1958.
- [30] G. L. Matthaei, "Design of wide-band (and narrow-band) bandpass microwave filters on the insertion loss basis", *IRE Trans. Microw. Theory Tech.*, vol. MTT-8, no. 11, pp. 580–593, Nov. 1960.
- [31] C. Y. Chang and T. Itoh, "A modified parallel-coupled filter structure that improves the upper stopband rejection and response symmetry", *IEEE Trans. Microw. Theory Tech.*, vol. 39, no. 2, pp. 310–314, Feb. 1991.
- [32] A. Riddle, "High performance parallel coupled microstrip filters", in *IEEE MTT-S Int. Microwave Symp. Dig.*, pp. 427–430, 1988.

- [33] D. M. Pozar, Microwave Engineering, 2nd ed. New York: Wiley, pp. 474–485, 1998.
- [34] T. Hirota, “Reduced-size branch-line and rat-race hybrids for uniplanar MMIC’s”, IEEE Trans. Microwave Theory Tech., Vol.38, No. 3, March 1990
- [35] G. Matthaei, L. Young, E. M. T. Jones, Microwave Filters, Impedance -Matching networks, and Coupling Structures, Artech House, pp.220.
- [36] I. Kang and J. Choi, “A new reduced-size lumped distributed power divider using the shorted coupled line pair”, Korea Electromagnetic Engineering Conference, vol.13, No.1, pp283-287, Nov. 2003.
- [37] Yi K.H. and Kang B.K. “Modified Wilkinson power divider for nth Harmonic Suppression”. IEEE microwave and wireless components. vol. 13. no. 5. pp.178-180, 2003
- [38] In-Ho Kang and Hai-Yan Xu, “Modified Wilkinson power divider for Multiple Harmonics Suppression”. International Journal of Navigation and Port Research, vol.29, No.7, September 2005



Acknowledgement

I would like to acknowledge a number of people who have helped me during the past two years. There is no way for me to finish this thesis without their supports and encouragements.

First and foremost, my greatest appreciation surely belongs to Prof. In-Ho Kang, who guided me through the M.S. program. His creativity, broad knowledge and insight into the circuit design helped me avoid going down wrong path and shortened the path to achieve the project goal. His energy and love of what he is doing inspires me a lot. I feel very grateful for his supervision both on the technical and the personal levels during my stay in Korea.

I would also like to express my sincere gratitude to the other professors of our school for their guidance. I am particularly grateful to my thesis committee members Prof. Young Yun and Prof. Dong-Kook Park for their time and valuable suggestions in guiding and reviewing my work. My acknowledgement will not be complete without mentioning the staff members of the Department of Radio Science and Engineering for their dedication and assistance.

I want to thank all the past and present members of the RF Circuit & System Lab, especially Mrs. Haiyan Xu and Mrs. Guan Xin, for their professional and personal supports. There is also my gratitude to all other friends at Korea Maritime University , especially Fangfang Jiang ,OOI Chew Yong, Li Jia and Lim Wei-nee, for the friendly environment and emotional supports. I will not forget the time we spent together before and in the future.

Additionally, I am deeply indebted to Prof. Ying-Ji Piao at Qingdao University. Without her recommendation, it is impossible for me to get this great opportunity to study in Korea.

Finally, I would like to dedicate this thesis to my family for their continued love and strong supports throughout all these years. You are always the persons who believe in and encourage me in all my endeavors, which is a contributing factor to any success I may achieve. Without these endless and priceless loves, it will never be possible for me to still live happily and accomplish my tasks. I feel great fortune to have you all accompany with me, only in this way, my life is complete and honorable.

